Design and optimisation of wheel-rail profiles for adhesion improvement

Journal:	*Vehicle System Dynamics*
Manuscript ID	NVSD-2015-0252.R1
Manuscript Type:	Original Paper
Date Submitted by the Author:	01-Dec-2015
Complete List of Authors:	Liu, Binbin; Politecnico di Milano, Mechanical engineering Mei, T X; University of Salford, School of Computing Science & Engineering Bruni, Stefano; Politecnico di Milano, Department of Mechanical Engineering
Keywords:	optimisation, wheel profile, contact, adhesion, Weibull distribution

Design and optimisation of wheel-rail profiles for adhesion improvement

B. Liu[a], T.X. Mei[b] and S. Bruni[a]

[a]Dipartimento di Meccanica, Politecnico di Milano, Via La Masa 1, Milano 20156, Italy
[b]School of Computing, Science and Engineering, University of Salford, Salford M5 4WT, UK

E-mail corresponding author: *binbin.liu@polimi.it*

Address for correspondence:

Binbin Liu
Dipartimento di Meccanica
Politecnico di Milano
Via La Masa 1
20156 Milano ITALY

Tel: +39 02 2399 8467
Fax: +39 02 2399 8460
e-mail: *binbin.liu@polimi.it*

Abstract

This paper describes a study for the optimisation of the wheel profile in wheel-rail system to increase the overall level of adhesion available at the contact interface, in particular to investigate how the wheel and rail profile combination may be designed to ensure the improved delivery of tractive/braking forces even in poor contact conditions. The research focuses on the geometric combination of both wheel and rail profiles to establish how the contact interface may be optimised to increase the adhesion level, but also to investigate how the change in the property of the contact mechanics at the wheel-rail interface may also lead to changes in the vehicle dynamic behavior.

Key words: optimisation, wheel profile, contact, adhesion, Weibull distribution

1. Introduction

The cross sections of the railway wheel and rail are referred to as profiles that are the basis of the contact geometry problem in wheel-rail system. Traditionally, the design of profiles has relied on the experience of engineers. More recently, the use of computer technology has led to the development of advanced techniques of profile design and optimisation. The profile optimisation can be treated as a single-objective geometry optimisation problem from the mathematical point of view or a more complicated multi-objective optimisation problem when geometric contact and vehicle dynamics are taken into account simultaneously from vehicle-track compound system point of view. In 1991, R. Smallwood *et al*. [1] developed a specific package for rail profile optimisation based on measured worn profiles by choosing three optimal objectives of low contact stress, minimized metal removal in grinding and vehicle stability. I.Y. Shevtsov *et al*. [2] employed a multipoint approximation based on response surface fitting to design an optimum wheel profile that matches a target rolling radius difference (RRD) function with the aim of improving vehicle stability and minimising wheel wear where the critical part is the selection of a proper RRD function. G. Shen *et al*. [3] proposed an inverse method by employing contact angles and rail profile information to form a target-oriented problem for the design of a wheel profile to reduce the flange wear and to increase the contact stiffness for the independent wheels of a tramcar. I. Persson *et al*. [4] applied genetic algorithms for the multi-objective optimisation of railway wheel profiles to reflect the importance of various factors including the maximum values of contact stress, lateral force on the track, derailment quotient and total wear and ride index. H. Jahed *et al*. [5] proposed a similar method used by I.Y. Shevtsov [2] and they chose a reduced set of generalized coordinates together with cubic spline curves in a linear programming formulation for the generation of profiles. The objective is to minimise the deviation of the geometric contact characteristics of the generated profiles from the target one, under the given vehicle and track characteristics. D. Cui *et al*. [6] proposed a direct numerical method to optimise the railway wheel profile based on the weighed normal gap between wheel and rail around their contact point to improve the distribution of the contact points, reduce the contact stress level, and decrease the wear and rolling contact fatigue (RCF). However, the methods mentioned above have aimed at improving the vehicle dynamic performances and/or reduction of contact forces/wear/RCF on curves. There has been

little attention to address the effect of profile design on the adhesion level in wheel-rail interface, which can present a serious problem for the effective operation of rail vehicles especially in poor contact conditions where the overall adhesion can be substantially reduced by external contaminants such as snow, moisture or tree leaves etc. Low adhesion conditions cause many problems for the scheduling and safety of railway networks around the world such as defects on wheels and rails, signals passed at danger, station platform overruns and even collisions [7, 8].

The aim of this work is therefore to study how wheel profiles may be designed to improve the adhesion characteristics between the wheel and rail, and to investigate the impact of the new design approach on the vehicle dynamic behaviours. It will mainly seek to demonstrate the general principle to increase adhesion limit from the profile re-design and optimisation.

2. Friction and adhesion

Adhesion in the railway field refers to the transmitted tangential force between wheel and rail due to creep. The adhesion coefficient is defined as the ratio of resultant tangential contact force over normal load for wheel-rail contact system as expressed in equation (1).

$$\mu = \frac{\sqrt{T_x + T_y}}{N} \tag{1}$$

where T_x and T_y denote the longitudinal and lateral tangential contact forces between the wheel and rail, respectively. Based on the data available from field measurements and laboratory experiments, the adhesion coefficient is typically assumed as a function of creepage as presented in Fig. 1.

FIGURE 1 TO APPEAR ABOUT HERE

It can be seen from Fig.1 that in order to ensure effective operation of railway vehicles and rail networks and to prevent wheel and rail from damages, an appropriate adhesion margin referred to the difference between adhesion limit and adhesion coefficient at the wheel-rail interface for delivering tractive/braking forces is essential.

For the railway wheel-rail contact, the development conditions of potential frictional properties are of particular interest and have been to taken into account in the commonly used mathematical models such as FASTSIM [9] and Polach's model [10]. The later is able to account for the so called falling friction and speed dependency of the creep-creep force relations and it is more often used for traction vehicle running on adhesion limit. E. Vollebregt [11] proposed an extension model of CONTACT [12] developed by Kalker in order to account for the effect of slip velocity and elastic third body layer on the friction coefficient. Y. Zhu *et al*. presented a numerical model in [13] for predicting wheel–rail adhesion under dry and lubricated conditions with measured 3D wheel–rail surfaces, and B. Allotta *et al*. [14] developed an adhesion model aimed at increasing the accuracy in

reproducing degraded adhesion conditions in vehicle dynamics by considering some of the main phenomena behind the degraded adhesion, namely the large sliding at the contact interface, the high energy dissipation, the consequent cleaning effect on the contact surfaces and the adhesion recovery due to the external unknown contaminant removal. These models attempt to improve the accuracy to same extent from different points of view. Nevertheless, the studies on the influence of contact geometry on the adhesion limit or friction coefficient are very limited. The investigations made for disc brake in paper [15] show that friction coefficient increase with the increase of the contact area of contact pair. Moreover, K. Six *et al*. [16] recently proposed a so-called ECF model which is able to take into account all observed effects from measurement regarding the adhesion coefficient including contact geometry.

The revealed relationship between the adhesion limit and contact geometry make it possible to relate the profile design to the adhesion characteristics in the wheel-rail system. This is the basis of the optimisation methodology for wheel profile to be proposed in the next section.

3. Profile optimisation considering adhesion characteristics in wheel-rail system

3.1 Optimisation methodology

As discussed above, none of the commonly used contact models is able to take the effect of the contact geometry on the adhesion limit into consideration. Therefore, a simplified alternative focusing on the influence of the contact geometry consequently the contact area on the adhesion limit is proposed based on the following analysis.

The research in reference [15] on the influence of geometric characteristics on static friction coefficient for elastic non-saturated in case of disk brake contact shows that while increasing contact area 1.5 times it becomes possible to increase the friction coefficient by 2.2%. Moreover, the results shown in reference [16] suggest that the relationship between the rail head radius and traction coefficient is nearly linear, while increasing the head radius of the rail by 2 times, the traction coefficient increases roughly by 20%, and obviously the contact area formed in the contact interface is a non-linear function of the radius for the twin-disc contact. The authors concluded that decreasing the contact area by reducing the rail head radius decreases the traction level significantly. In addition, many experiments performed as described in [17, 18] have proven that the adhesion coefficient decreases with the increase in contact pressure which has an inverse proportionality to the size of the contact patch. Therefore, for the quantitative analysis in this study, a simplified linear relationship between the adhesion limit and the contact area is assumed in order to demonstrate in principle the potential of adhesion improvement of the proposed approach.

The choice of optimisation algorithms mainly depends upon the optimisation objective. The multi-objective optimisation method is quite popular in wheel profile design in order to consider as many factors as possible from the complete system point of view, although the complexity and calculation effort increase considerably at the same time and there is

no guarantee that the optimal solution can be found in some cases. The main objective of this study is to increase the overall level of adhesion available at the contact interface by wheel profile optimisation. The assumption that the adhesion limit is proportional to the contact area makes it possible to formulate the optimisation problem in question as a single-objective optimisation which is achieved by adjusting the distribution of contact area over the potential contact region on the wheel. It means a more uniform distribution of the contact area over the contact band of the wheel is the preferred solution in this case.

The mathematical description of the profile is the basis of a numerical optimisation process. In order to maintain some required geometric characteristics of the wheel profile depending on the aim of design, some special mathematic techniques have been developed [4, 5, 19]. As an alternative, a new optimisation approach is proposed based on the fact the contact distribution will tend to be uniform after a new profile experiences wear in practice. The idea is to simulate the wear process occurring on the wheel profile in reality. The wear form called removal function in this paper is assumed to comply with Weibull distribution function as expressed in equation (2).

$$f(x) = k\frac{\beta}{\mu}\left(\frac{x-\gamma}{\mu}\right)^{\beta-1} e^{-\left(\frac{x-\gamma}{\mu}\right)^{\beta}} \tag{2}$$

where k is global scaling factor, β is the shape parameter, μ is the scale parameter and γ is the location parameter, and x is the lateral coordinate of the candidated wheel profile. Some cases generated from equation (2) with typical parameters are shown in Fig.2.

FIGURE 2 TO APPEAR ABOUT HERE

The introduction of the removal function in the proposed method simplifies this problem as the optimisation region can be chosen flexibly whilst the other main geometric characteristics remain unchanged throughout the optimisation. The profile can be updated by subtracting the removal function from the original profile.

To achieve an uniform contact distribution, the area of each contact patch needs to be calculated at the potential contact region in normal operational conditions of the wheelset. To this end, a code has been developed in MATLAB for contact point searching and contact patch estimation based on the rigid-contact algorithm and the non-elliptic contact method proposed by W. Kik *et al*.[20] The optimisation problem can be simply expressed in the form of equations (3) and (4).

$$maximize \;\; A_{RMS} = \sqrt{\frac{1}{\mathrm{n}}\sum_{\mathrm{i}=1}^{\mathrm{n}} A_i^2\left(\sum_{j=1}^{m} f_j(x), y_i\right)} \tag{3}$$

$$subject\ to \;\; -8 \le y_i \le 5\ (mm) \tag{4}$$

where n is the number of contact patch over the potential contact region on the wheel profile, A_i is the contact area of the i-th contact patch, $f(x)$ is the removal function refer to Equation (2), and y_i is the lateral displacement of the wheelset, and positive value correspond to the wheelset moving towards the right side of the track. There are a total of 5 different parameters for tuning in Equation (2) and m number of removal functions are considered in the optimisation. Therefore, the number of variables involved in the optimisation is $5\times m$. In addition, the wheelset lateral displacement is included as a constraint. The experience in heavy-haul traffic shows the ideal friction coefficient between the wheel and rail is high level over wheel tread and low level at wheel flange [21]. From this fact, the optmization region is chosen according to equation (4) to obtain optimised adhesion level by optimizing the wheel tread and reverse the flange part of the original profile.

The optimisation problem (3) is solved by using the built-in function *fminsearch* in MATLAB, and the constraint equation (4) is applied externally by fixing the boundary of the lateral coordinate of the wheel x in equation (3). The function *fminsearch* uses a derivative-free method to find the unconstrained minimum of a multivariable objective function starting at an initial estimate, thereby the computational cost and number of iterations required depend on the initial estimats, and the values used here are as follows: k_1=0.7, β_1=4.5, μ_1=22, γ_1= -10, k_2=1.2, β_2=4.5, μ_2=35, γ_2=20. The flow chart of the wheel profile optimisation procedure is presented in Fig. 3.

FIGURE 3 TO APPEAR ABOUT HERE

3.2 Optimisation results

The typical wheel-rail profile combination of S1002/UIC60 has been chosen as the candidate to be optimised. The track gauge is 1435 mm with the rail inclination of 1:40 and the wheel flange back spacing is 1360 mm. A series of constant normal load of 50, 80 and 100 kN are applied to the contact patch. For simplicity, the rail profile is considered to be constant only the wheel profile is subjected to change. The contact characteristics of the original profile combination are show in Fig.4.

FIGURE 4 TO APPEAR ABOUT HERE

It can be seen from Fig.4 (c) that the variation of the contact area with respect to the lateral displacement of the wheelset is substantial, but the variation pattern of the contact area is largely independent of the normal load applied on the contact patch. Similar conclusion can be drawn for the maximum pressure shown in Fig.4 (d).

As mentioned above, the removal function can be a single Weibull function or a summation of functions using a number of parameters to form various wear patterns such as a single peak or double peaks appearing on the tread of wheel depending on the requirements of optimisation. Two case studies have been performed for the removal function formed by the single- (m=1, cf. Equation 3) and double-Weibull (m=2) functions in optimisation respectively, and the results are shown in Fig.5.

FIGURE 5 TO APPEAR ABOUT HERE

It can be seen from Fig.5 (a), (c) and (e) that the contact point distribution becomes more uniform after optimisation which is favourable for preventing wear and RCF. Fig.5 (b) shows that only the segment close to flange root of the wheel profile has been changed by the single-Weibull removal function method, whereas the double-Weibull removal function method further optimises the profile in a wider region. Consequently, more uniform contact distribution in the sense of contact point and contact area by the double-Weibull optimisation is provided in the region on wheel covered by -5 mm to 5 mm lateral displacement of the wheelset as shown in Fig.5 (d). Fig.5 (f) shows that the optimised profile combination possesses low equivalent conicity before the flange contact which implies the optimisation improves the wheelset hunting stability as well. It is clear that the optimised profile from the double-Weibull removal function method is preferable in the context of this research. Therefore, it will be used in the following sections for further investigation and simply called optimised profile in the rest of this paper. It is worth mentioning that, whilst it may be possible to further improve the contact areas and the distributions of the contact areas by extending the removal function to the summation of more Weibull functions with more design variables and complexities taken into account (or other optimisation methods), this optimised profile will be used for the study below to demonstrate the principle of improving the adhesion margins for traction and braking.

4. Dynamic simulation

The optimised profile has been obtained by considering the local contact conditions, it is necessary to investigate the effect of the optimised profile on the dynamics responses at a complete vehicle system level. To this end, a three-dimensional model of a passenger vehicle has been built in the multi-body dynamic system (MBS) simulation package SIMPACK. The model consists of a carbody and two bogies with two stages of suspension systems, totalling 11 rigid bodies with 46 degrees of freedom. The axle load is 10 tonnes and the type of the vehicle can be switched from a trailing vehicle to a traction vehicle by activating the tractive effort applied on the first axle of the first bogie. The contact forces are calculated by using FASTSIM, and different wheel profiles and contact calculation methods are used for the purpose of comparison. It is worth noting that the FASTSIM algorithm is used even for traction simulation instead of the Polach's method which is more suitable for modelling creep over saturation because the current work is focusing on the contact properties prior to the saturation phase. The rails are inclined at

1:40 and only the tangent track and curve sections are considered throughout all the simulations.

4.1 Hunting stability

The stability analysis of the vehicle has been run to find the vehicle critical speed prior to assigning more simulation cases for curving negotiations. A lateral disturbance with a magnitude of approximately 10 mm is set on the right side rail of an ideal track at the distance of around 50 m away from the starting position to excite lateral instability of the vehicle. The vehicle is running on this track starting at a very high speed with a deceleration of 1 m/s^2. The speed at which the lateral displacements of the wheelset decay in Fig. 6 is assumed to be the critical speed of the vehicle for the purpose of this work. The lateral displacement of the wheelset against the vehicle's speed before and after the profile optimisation are shown in Fig.6.

FIGURE 6 TO APPEAR ABOUT HERE

The simulation results show that the lateral displacement of wheelset decay at the speed of approximately 240 and 250 km/h, respectively for the vehicle equipped with original and optimised profiles. It suggests that the optimised profile can slightly improve the system stability and this result agrees with the equivalent conicity analysis shown in Fig.5 (f).

4.2 Curving performance

Based on the assumption made in section 3.1 that the adhesion limit is proportional to the contact area at the wheel-rail interface the classical FASTSIM algorithm extended with variable adhesion limit as a function of contact area is used for tangential contact force calculation. By doing so, the effect of the wheel profile on the adhesion characteristics may be considered. This is obviously a simplification as the actual relation may well be quite nonlinear, but it should be provide useful insight into the potential improvement offered by the proposed profile optimisation for the provision of tractive/braking effort.

With reference to Fig.5 (d), by choosing the maximum contact area obtained in case of original profile combination as reference corresponding to an adhesion limit of 0.35, the adhesion limits as function of lateral displacement of the wheelset can be calculated by proportional scaling as shown in Fig.7 (a). It can be seen that the adhesion limit obtained at the wheelset central position is lower than the original profiles. However, it should be kept in mind that the contact area at the central position, i.e. on straight track, of the original profiles is much larger than that at other positions and therefore the reduced margin to saturation at this position after the optimisation is not expected to make a significant adverse effect on the availability of the adhesion for traction and braking. The proposed optimisation will only reduce the conservativeness of the original design. In order to incorporate the variable adhesion limit into MBS simulation, it is necessary to

convert the functions shown in Fig.7 (a) to the relationship between the adhesion limit and *y*-coordinates of wheel profile as requested in SIMPACK as shown in Fig.7 (b).

FIGURE 7 TO APPEAR ABOUT HERE

The curving negotiation simulation was carried out under the operating conditions of the vehicle passing representative curves of different radii with a constant speed. More details on the simulation cases are listed in Table 1.

TABLE 1 TO APPEAR ABOUT HERE

The simulation cases 1-3 in Table 1 are designed for vehicle dynamics analysis and case 4 for traction simulation. The time histories of adhesion coefficient of the wheelset 1 for cases 1 and 4 with the two different wheel profiles are presented in Fig.8.

FIGURE 8 TO APPEAR ABOUT HERE

It can be seen from Fig.8 that the available adhesion margins (shown in Fig.8 by vertical arrows) vary with the track input. On the tangent section, the margin is broader than that on the curve, and the original profile obtain broader adhesion margin at all times compared with the optimised profile in the tangent sections. The optimised profile can improve the adhesion margin available at the wheel-rail interface as the applied tractive effort results in the saturation on the full curve section in case of the original profile and the optimised profile is shown to avoid this problem, seen in Fig.8(c).

In order to investigate the effect of the profile optimisation on the adhesion level with different track inputs, the comparisons of adhesion level before and after the profile optimisation on the full curves for all cases in Table 1 are shown in Fig.9.

FIGURE 9 TO APPEAR ABOUT HERE

It can been seen from Fig.9 (a) that the adhesion limit is increased for the wheelsets 1 and 4 after the profile optimisation, and significantly improvement in the sense of the available adhesion margins (shown by the blank part of the histogram in the figures),

approximately 200% is observed for the left (outer) wheels where the creep force is approaching the saturation. In contrast, the available adhesion margin for the wheelsets 2 and 3 slightly decrease with the optimised profiles, but the creep forces are far away from saturation in these cases.

With reference to Case 1 shown in Fig.9 (a), Case 2 shown in Fig.9 (b) represents the vehicle running at the same speed on a curve with a smaller radius. For Case 2, the available adhesion margin is broadened for all wheels after the profile optimisation by approximately a maximum of 200% and minimum of 16%, except the left wheel of wheelset 1 with a decrease of 20%.

Compared with Case 2, Case 3 shown in Fig.9 (c) represents the vehicle running at the same speed with cases 1 and 2 on a curve with a further reduced smaller radius. It can be seen that the creep reaches the limit on the left (outer) wheels of the wheelsets 1, 2 and 3 with original profiles, but not the case after the profile optimisation. It means the optimised profile would be able to reduce the occurrence of wheel sliding in this situation.

Referring to Case 1 shown in Fig.9 (a), Case 4 shown in Fig.9 (d) represents the same condition except the tractive effort is included for the vehicle by applying a torque on the first axle (wheelset 1). It can be observed that the left (outer) wheel of the wheelset 1 with the original profile reaches the saturation due to the torque applied, whilst for the same wheel with the optimised profiles there is still some margin from the limit. The adhesion coefficient of the right wheel of the wheelset 1 in Case 4 decreases with respect to Case 1 without power, the tractive effort has an influence on the adhesion of wheelset 2 as well but not on the other wheelsets.

It can be concluded from Fig.9 that the optimised profile is capable of improving the adhesion level considerably when the vehicle runs through a curve, providing increased margins for the application of tractive effort in addition to the contact forces necessary for negotiating curves.

The variation of adhesion margin with track condition can be explained with reference to the dynamic behaviour of the wheelsets. The time histories of the displacements of wheelsets for cases 1 and 3 are presented in Fig.10.

FIGURE 10 TO APPEAR ABOUT HERE

It can be observed for Case 1 from Fig.10 (a) and (b) that the wheelsets are moving towards the outer rail from track central position to approximately -3.5 mm laterally when the vehicle runs through the curve. At the beginning of the simulation, the vehicle is running on the tangent section of the track and the wheelset does not move laterally. The adhesion limit of the wheel with the original profile is higher than that of the

optimised one because of the relationship between adhesion limit and lateral displacement of wheelset shown in Fig.7 (a) that the adhesion limit of the original profile is larger than the optimised one in the vicinity of the central position of the track approximately in the range of -2 to 2 mm. This can change if the track irregularities are considered as the wheelsets respond to the random lateral displacement of the track. When the vehicle is running on the transition gradually approaching to the full curve, the lateral displacement of the wheelset keeps growing until it reaches approximately -2 mm the adhesion limit curves obtained from original and optimised profiles come across at one common point which is consistent with the figure shown in Fig.7 (a). Similar fashion of the variation is also shown in Fig 10 (c) and (d) for Case 3, but larger magnitudes of lateral displacements of the wheelsets are obtained due to the smaller curve radius. These results can also explain the decrease of the adhesion level shown in Fig.9 in some cases.

It should be noted that the wheel-rail profiles are optimised to improve the general adhesion conditions across the contact points of the wheels, but it is possible to optimise the profiles differently, e.g. to increase the adhesion margins on the tangent track by focusing on the contact region of the contact surfaces.

These results have shown that the optimised profile is capable of increasing the adhesion level available in the wheel-rail interface as expected. But it still needs to investigate how the change in the property of the contact geometry and contact mechanics at the wheel-rail interface may also lead to changes in the vehicle dynamic behaviour. To this end, some parameters important to safety and maintenance issues when a railway vehicle is running on a curve are considered. They are wear measured by frictional work, derailment quotient, contact stress and lateral track shift force. The maximum values in the time histories of these parameters are summarised in Table 2.

TABLE 2 TO APPEAR ABOUT HERE

It can be observed from Table 2 that, for the cases considered, the frictional work increases by applying the optimised profiles due to the combined effect of the increased adhesion coefficient and contact area after the profile optimisation. However, the maximum contact pressure decreases considerably after the profile optimisation which would be of beneficial for reducing the occurrence of surface damage. The best compromise between wear and RCF of a wheel for extending its useful life cannot be easily determined, however, these two damage effects can be taken into account simultaneously in the optimisation problem, for instance [22], which is out of the scope of this study, more details on the wear or RCF can be found in references [23-25]. Moreover, the wheel profile type has marginal effect on derailment quotient and lateral track shift force.

5. Conclusions

A simple and flexible optimisation method for the railway wheel profile by inclusion of the Weibull distribution function has been proposed to increase the overall level of adhesion available at the contact interface in the paper. The geometric analysis of wheel and rail profiles and the non-elliptic contact estimation have been carried out to ensure the optimised profile is able to provide suitable contact geometry and contact mechanics characteristics. The effect of the contact geometry on the adhesion has been taken into account in the simulation. Finally, the obtained optimised profile has been incorporated into a complete vehicle MBS model so as to evaluate the dynamic behavior of the vehicle system after the profile optimisation. Based on the analysis of the results obtained in this study the following conclusions can be drawn.

1) Wheel profiles may be re-designed to improve the adhesion margins available at the wheel-rail interface. Different optimal profiles can be designed according to the operational conditions. The same situation can be expected for rail profile design as well. The optimised profile could be a new contribution for dealing with the low adhesion problems.
2) The rail vehicle dynamic properties are not adversely affected after profile optimisations, such as the hunting stability and in some cases are actually improved, such as the lower contact pressure when the vehicle passing curves. The lower contact pressure, larger contact area and higher adhesion coefficient after the profile optimisation have contradictory effects on the wear. Therefore, a trade-off needs to be found in this regard.
3) Although the profiles used in the study may not necessarily be 'the best' and the method to take into account the adhesion may not be perfect, the general observations should stand. A new direction has been pointed out for dealing with poor adhesion problems, although more precise quantitative analysis needs to be carried out with more advanced optimisation and adhesion modeling techniques for further study.

References

[1] R. Smallwood, J.C. Sinclair and K.J. Sawley, An optimisation technique to minimize rail contact stresses, Wear, 1991;144: 373-384.
[2] I.Y. Shevtsov, V.L. Markine, C. Esveld, Optimal design of wheel profile for railway vehicles, Wear, 2005; 258 :1022-1030.
[3] G.Shen, J.B.Ayasse, H.Chollet, I.Pratt, A unique design method for wheel profiles by considering the contact angle function, Proceedings of the Institution of Mechanical Engineers, Part F: Journal of Rail and Rapid Transit. 2003;217:25-30.
[4] I.Persson, S.D.Iwnicki, Optimisation of railway profiles using a genetic algorithm, Vehicle System Dynamics. 2004;41:517-527.
[5] J. Hamid, F. Behrooz, A. Mohammad et al. A numerical optimisation technique for design of wheel profiles. Wear 2008; 264: 1–10.
[6] D. Cui, L. Li, X. Jin, X. Li, Optimal design of wheel profiles based on weighed wheel/rail gap, Wear. 2001;271 :218-226.
[7] Oscar Arias-Cuevas, Low Adhesionin the Wheel-Rail Contact, PhD thesis 2010, Delft University of Technology, Delft, the Netherlands.
[8] J. Thommesen, N. J. Duijm, and H. B. Andersen, Management of low adhesion on railway tracks in European countries, Kgs. Lyngby: DTU Management Engineering, 2014.
[9] J.J. Kalker. A fast algorithm for the simplified theory of rolling contact. Vehicle System Dynamics, 1982;11:1-13.

[10] O. Polach, Creep forces in simulations of traction vehicles running on adhesion limit. Wear. 2005; 258:992– 1000.
[11] EAH Vollebregt. Numerical modeling of measured railway creep versus creep-force curves with CONTACT. Wear. 2014; 314:87–95.
[12] J.J. Kalker, On the rolling contact of two elastic bodies in the presence of dry friction. Dissertation TH Delft, Delft (1967)
[13] Y. Zhu, U. Olofsson and A. Söderberg, Adhesion modeling in the wheel–rail contact under wet conditions using measured 3D surfaces, Proceedings of IAVSD 2011: International Symposium on Dynamic of Vehicles on road and tracks, Aug 14-19, 2011, Manchester, UK.
[14] B. Allotta, E. Melin, A. Ridolfi, and A. Rindi, Development of an innovative wheel-rail contact model for the analysis of degraded adhesion in railway systems, Tribology International, vol. 69, pp. 128-140, 2014.
[15] Oksana Sergiyenko, Yuriy Osenin, An influence of geometrical characteristics of frictional elements on the effectiveness of disk brake, TEKA Kom. Mot. Energ. Roln. OL PAN, 2009; 9: 285-289.
[16] K. Six, A. Meierhofer, G. Müller & P. Dietmaier. Physical processes in wheel–rail contact and its implications on vehicle–track interaction, Vehicle System Dynamics. 2015; 53:5, 635-650, DOI: 10.1080/00423114.2014.983675
[17] Sinclair, J., Friction Modifiers, in "Vehicle Track Interaction: Identifying and Implementing Solutions", IMechE Seminar, February 17th, 2004.
[18] L. Deters and M. Proksch, Friction and wear testing of rail and wheel material, Wear. 2005;258:981-991.
[19] J. Santamaria, J. Herreros , E. G. Vadillo & N. Correa. Design of an optimised wheel profile for rail vehicles operating on two-track gauges, Vehicle System Dynamics, 2013, 51:1, 54-73, DOI: 10.1080/00423114.2012.711478.
[20] W. Kik, and J. Piotrowski, A fast approximate method to calculate normal load at contact between wheeland rail and creep forces during rolling. I. Zobory (Ed.), Proceedings of 2nd Mini-conference on contact mechanics and wear of rail/wheel systems. Budapest, 1996.
[21] H. Harrison, The development of a low creep regime, hand-operated tribometer, Wear.2008; 265 :1526-1531.
[22] H.Y. Choi, D.H. Lee, and J. Lee, Optimization of a railway wheel profile to minimize flange wear and surface fatigue. Wear. 2013; 300:225-233.
[23] G. Donzella, A. Mazzù, and C. Petrogalli, Competition between wear and rolling contact fatigue at the wheel-rail interface: some experimental evidence on rail steel. Proceedings of the Institution of Mechanical Engineers, Part F: Journal of Rail and Rapid Transit, 2009;223: 31-44, DOI: 10.1243/09544097JRRT161.
[24] J. Tunna, J. Sinclair, and J. Perez, A Review of wheel wear and rolling contact fatigue. Proceedings of the Institution of Mechanical Engineers, Part F: Journal of Rail and Rapid Transit, 2007;221 : 271-289, DOI: 10.1243/0954409JRRT72.
[25] A. Ekberg, E. Kabo and H. Andersson, An engineering model for prediction of rolling contact fatigue of railway wheels. Fatigue & Fracture of Engineering Materials & Structures 2002;25: 899-909, DOI 10.1046/j.1460-2695.2002.00535.x.

Table 1 Simulation cases

No.	Speed [km/h]	Radius [m]	Non-compensated acceleration [m/s^2]	Vehicle type
1	180	3000	0.31	trailing
2	180	2000	0.73	trailing
3	180	1500	1.14	trailing
4	180	3000	0.31	traction

Table 2. Main parameters for curving performance

Case No.	Frictional work of vehicle [J]		Derailment quotient of wheel		Contact pressure [MPa]		Track shift force [kN]	
	ori.	opt.	ori.	opt.	ori.	opt.	ori.	opt.
1	1802	1840	0.09	0.09	1300	900	10	10
2	3512	4012	0.15	0.15	1350	1047	15	15
3	6023	6823	0.21	0.20	1784	1395	20	21
4	2400	2400	0.09	0.09	1300	900	17	17

List of Figures

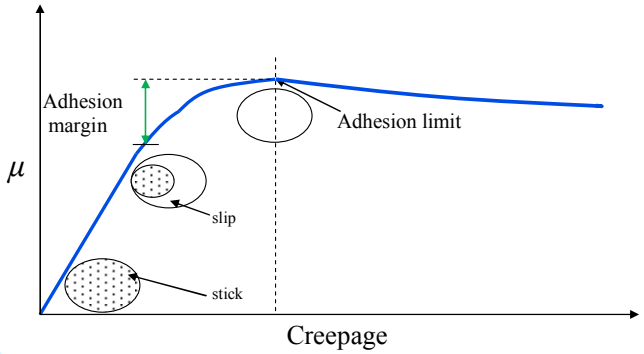

Fig.1 Adhesion variation with respect to creepage

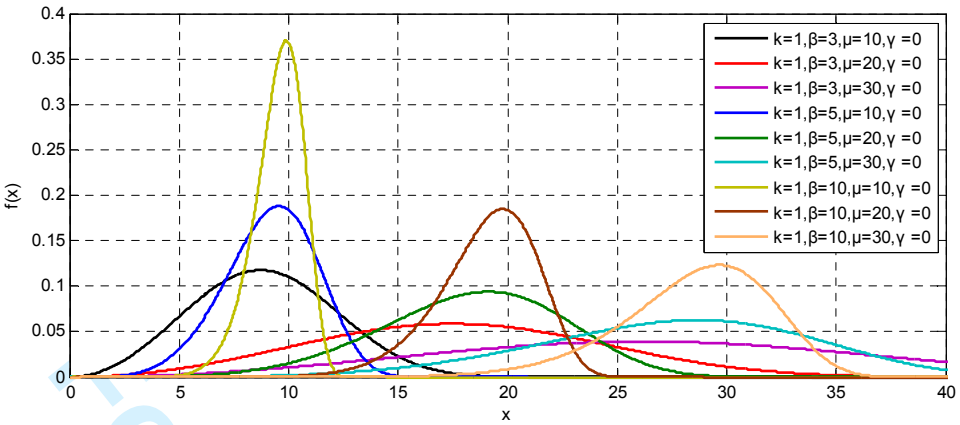

Fig.2 Typical Weibull curves

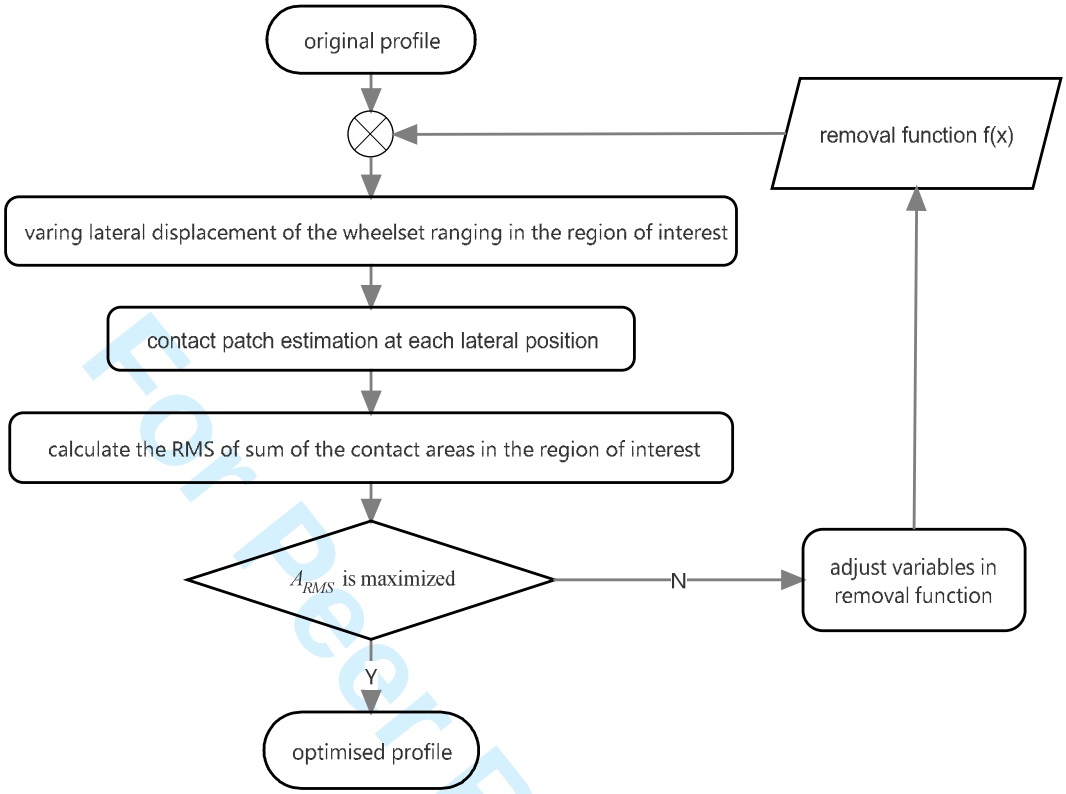

Fig.3 Flow chart of optimisation procedure

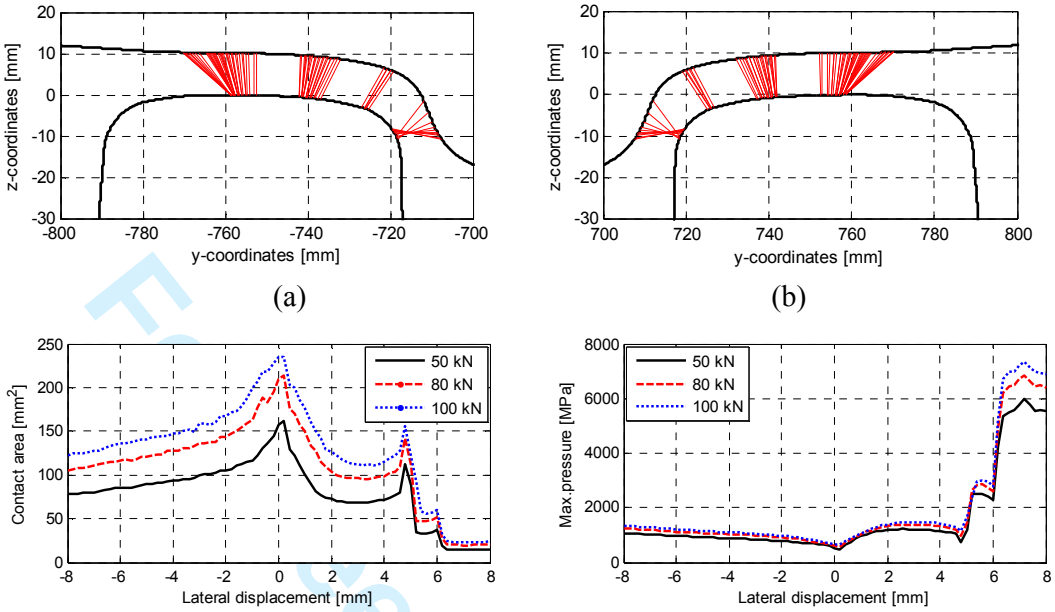

Fig.4 Contact characteristics under new S1002/UIC60 combination: contact point distribution on the left (a) and (b) right wheel-rail pair , contact area (c) and maximum pressure (d) variation against to lateral displacement of the wheelset.

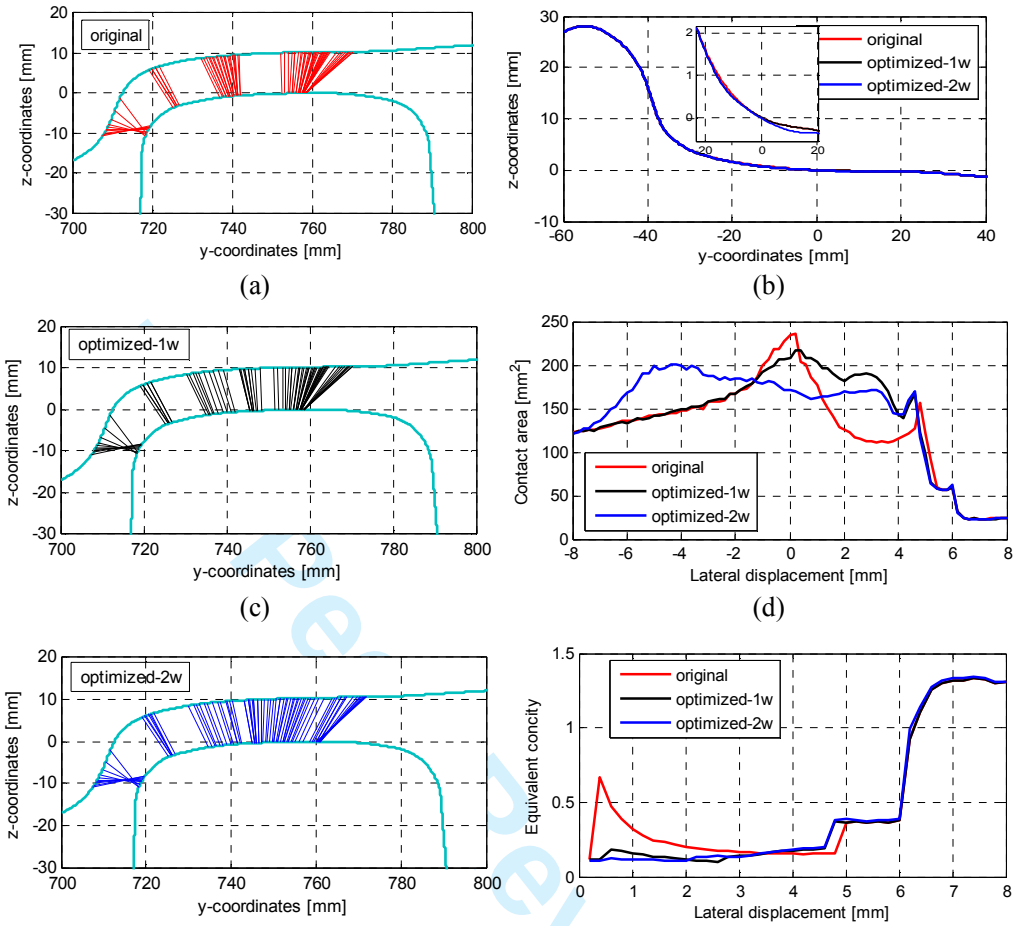

Fig.5 Contact point distribution generated by original profile (a), single-Weibull optimised profile (c) and double-Weibull optimised profile (e), and profiles before and after optimisation (b) with zoomed inset, contact area (d) and equivalent conicity (f) in function of lateral displacement of the wheelset, respectively.

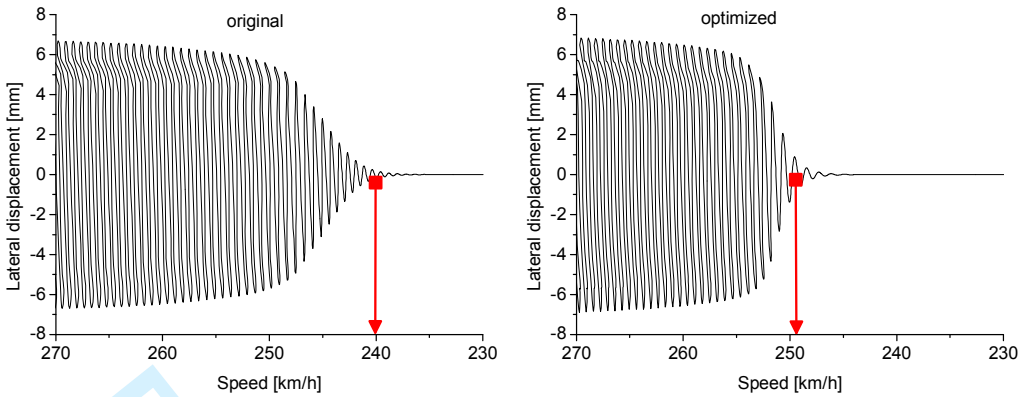

Fig.6 Lateral displacement of wheelset with original profile (left) and optimised profile (right)

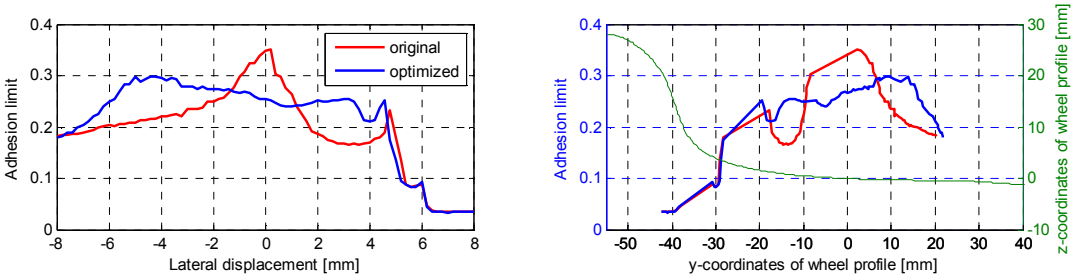

(a) (b)

Fig.7 Adhesion limit vs. lateral displacement (a) and y-coordinates of wheel profile (b)

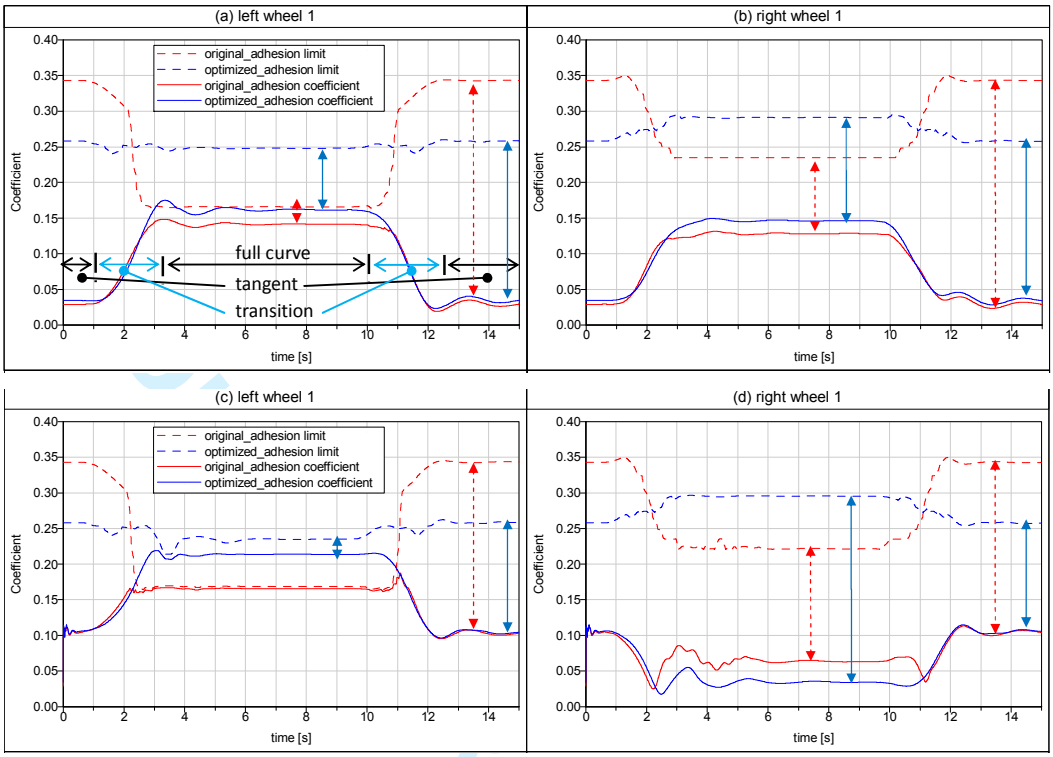

Fig.8 Adhesion characteristics on curve: left (a) and right (b) wheel of wheelset 1 for Case 1, and left (c) and right (d) wheel of wheelset 1 for Case 4.

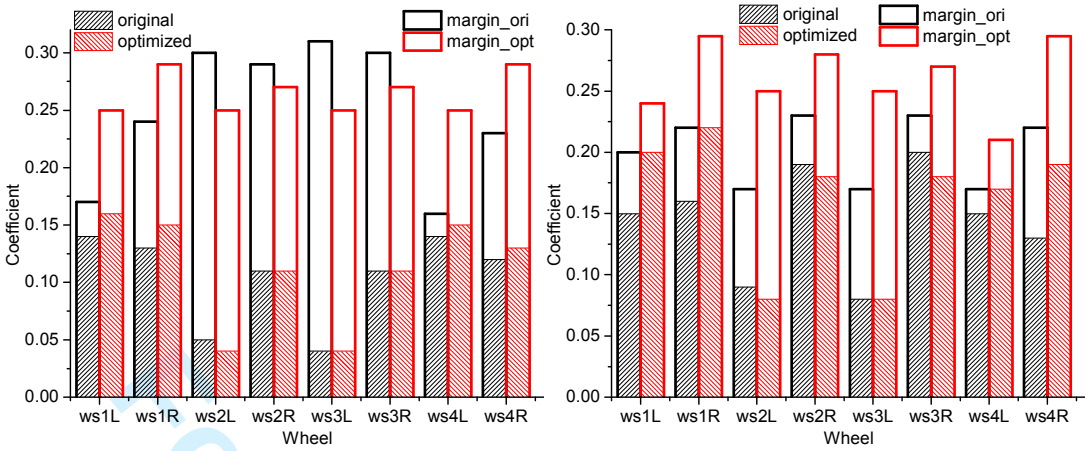

(a) Case 1 (b) Case 2

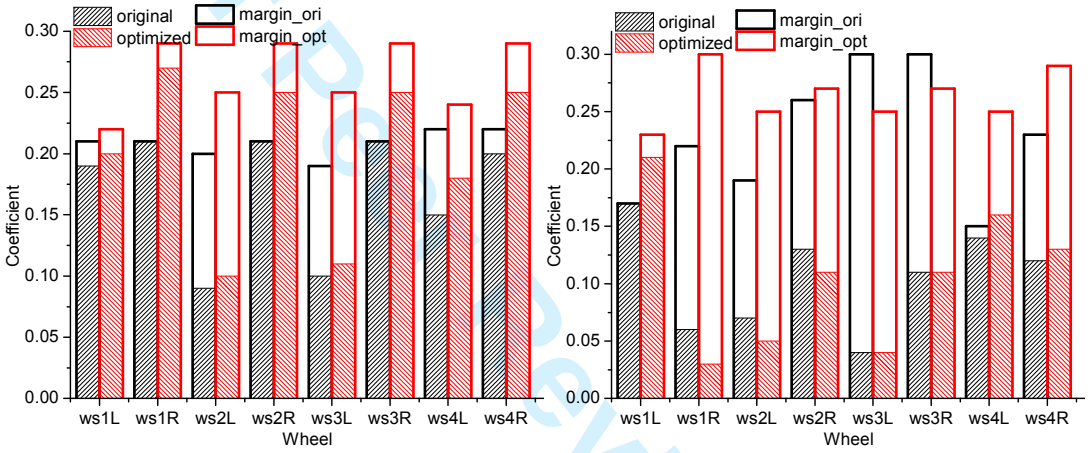

(c) Case 3 (d) Case 4

Fig.9 Adhesion level obtained from simulation for Case 1 (a), Case2 (b), Case 3 (c) and Case 4 (d).

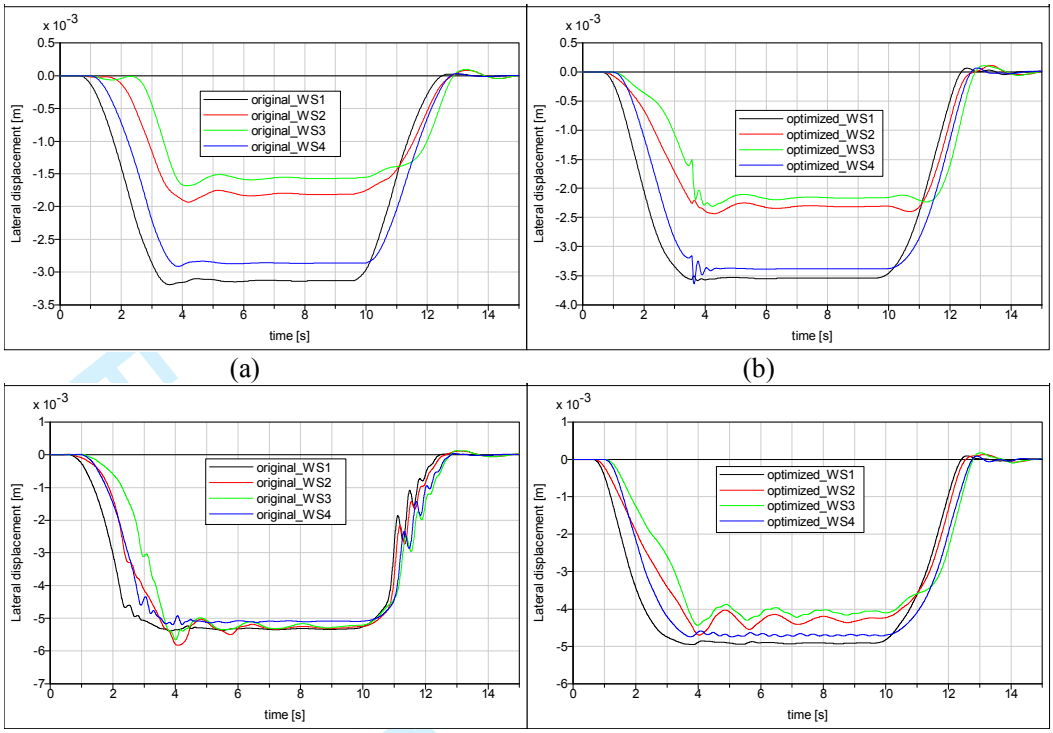

Fig.10 Lateral displacement of wheelsets calculated with (a) original and optimised profile (b) for Case 1 and Case 3 with original (c) and optimised profile (d).